Original Article

Integrated hazard assessment of rockfall incidents in the Cap Aokas Cliff Region

Zohra LADJEL[1,2] https://orcid.org/0009-0002-6074-7969; e-mail: ladjelzohra19@gmail.com

Farid ZAHRI[1,3,4] https://orcid.org/0009-0007-5183-9534; e-mail: zahrifarid@yahoo.fr

Riheb HADJI[1,3,4]* https://orcid.org/0000-0002-9632-0812; ✉e-mail: hadjirihab@yahoo.fr

Younes HAMED[4,5] https://orcid.org/0000-0001-7451-4459; e-mail: hamed_younes@yahoo.fr

Karim ZIGHMI[1,3,4] https://orcid.org/0009-0008-1869-0261; e-mail: zighmi.karim19@gmail.com

Kaddour BENMARCE[1,3,4] https://orcid.org/0000-0001-5484-424X; e-mail: kaddour.benmarce.24@gmail.com

*Corresponding author

1 Department of Earth Sciences, Institute of Architecture and Earth Sciences, Ferhat Abbas University, Setif 19137, Algeria

2 Unit of Emerging Materials Research, Ferhat Abbes University, Sétif 19137, Algeria

3 Laboratory of Applied Research in Engineering Geology, Geotechnics, Water Sciences, and Environment, Ferhat Abbas University, Setif 19137, Algeria

4 International Association of Water Resources in the Southern Mediterranean Basin, Gafsa 2112, Tunisia

5 Department of Earth Sciences, Faculty of Sciences, University of Gafsa, Gafsa 2112, Tunisia

Abstract: Rock fall accidents in mountainous cliff areas have significant consequences for human life and transportation. This study aimed to evaluate the rockfall hazard in the Cap Aokas cliff region located along the northeast coast of Algeria by identifying the key factors contributing to rockfall occurrence. We employed a combination of kinematic analysis, Matterocking method, and 3D trajectory simulations to determine zones that are susceptible to rockfall mobilization. By using a probabilistic and structural approach in conjunction with photogrammetry, we identified the controlling factors. The kinematic analysis revealed the presence of five discontinuity families, which indicated both plane and wedge failure modes. The 3D trajectory simulations demonstrated that the falling blocks followed the stream direction. We then validated the susceptibility maps generated from the analysis using aerial photos and historical rockfall events. The findings of this study enhance our understanding of rockfall phenomena and provide valuable insights for the development of effective strategies to mitigate rockfall hazards.

Keywords: Trajectory simulations; Probabilistic analysis; Structural approach; Rockfall hazard; Cap Aokas cliff

1 Introduction

Rockfalls pose significant geological hazards, often resulting in fatalities and substantial damage to property and infrastructure (Cruden and Varnes 1996;

Volkwein et al. 2011; Palau et al. 2013; Ferrari et al. 2016; Dahoua et al. 2018; Kallel et al. 2018; Corominas et al. 2019; Besser et al. 2021). Broad researches (Jiang et al. 2020; He et al. 2021) have underscored the necessity of comprehending the causes and dynamics of rockfalls to accurately evaluate hazards and formulate effective mitigation strategies (Ansari et al. 2018; Taib et al. 2023a,b, 2024). While analyses of the economic impact of rockfalls are abundant in the United States and Europe, research in Africa remains limited, highlighting a critical need for enhanced mitigation measures and research endeavors on the continent (Zeqiri et al. 2019; Mahleb et al. 2022; Brahmi et al. 2023).

In the mountainous regions of North Algeria, managing mass wasting risks is paramount, given disastrous incidents and the unpredictable nature of the phenomenon (Hadji et al. 2013, 2014; Achour et al. 2017; El Mekki et al. 2017; Dahoua et al. 2017; Manchar et al. 2018; Mahdadi et al. 2018; Anis et al. 2019; Kerbati et al. 2020; Fredj et al. 2020; Saadoun et al. 2020; Boubazine et al. 2022; Asmoay and Mabrouk 2023). This urgency was tragically underscored by an event on February 25, 2015, in Aokas region (NE Algeria), resulting in the loss of seven lives. This site has been a hotspot for rockfall occurrences over the past two decades, marked by the unpredictable distribution of zones where rock blocks detach (Karim et al. 2019). Dorren et al. (2013) have advocated for a three-tiered approach to rockfall analysis: D1 for mapping susceptibility, D2 for mapping hazards, and D3 for addressing risks.

Various methodologies, such as RES, RHAP, LPC, Matterocking, HGR, and trajectory analysis, are employed for rockfall hazard assessment, each tailored to specific objectives and levels of detail required (Hudson 1992; Descoeudres 1997; Regione 2000; Vengeon 2001; Depountis et al. 2020). However, adopting a deterministic approach to identify mobilization zones and track rock block propagation faces challenges due to the stochastic distribution of discontinuities on cliffs. One alternative approach integrating statistical and probabilistic treatments of discontinuities offers a practical solution (Jaboyedoff et al. 1996; Hantz et al. 2002).

This study delves into analyzing the geo-mechanical properties of rock mass discontinuities to grasp the structural attributes of rock formations (Jaboyedoff et al. 2007). Leveraging the Matterocking method renowned for spatial trajectory evaluations, a probabilistic model is applied (Jaccard et al. 2020). Research encompasses data preparation for kinematic analysis, identifying starting scenarios based on structural configurations and topography, simulating block trajectories, and assessing rockfall hazards.

Through the utilization of the structural arrangement of rock masses, this integrative model enables the thorough evaluation of rockfall hazards. This methodology holds promise for identifying potential failure zones along rocky cliffs in North Africa and Mediterranean basin countries.

2 Material and Methods

2.1 Study area

This study area encompasses the Aokas region, along the Mediterranean coastline (36°38'39''S, 5°14'24''E-5°13'30''E, Fig. 1). This region is characterized by the northern cliff of the Cap Aokas Mountain, with the national road RN°9 running through it. Notably, at the eastern extremity of this slope, an underpass tunnel has been constructed beneath the road. However, it's imperative to highlight that this road was closed off due to recurring rockfall incidents in both 2005 and 2015 (Fig. 2). This study area is positioned within the Western Babors mountain chain, more precisely within the Gouraya-Barbacha unit, (Chibani et al. 2022). Geologically, the carbonatic ridge of this region is underlain by Jurassic formations, (Tamani et al. 2019). The primary rock
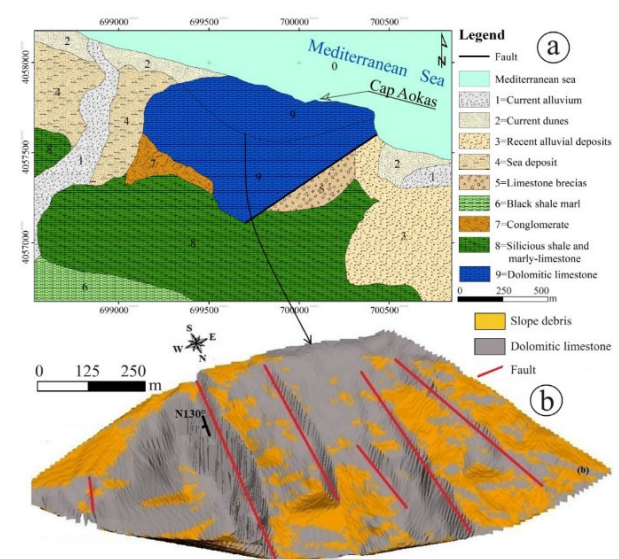

Fig. 1 (a) Geologic map of the study site; (b) Lithology of the cliff.

Fig. 2 Recurring rockfalls from the rocky cliffs of Cap Aokas.

type comprising the cliff consists of Liassic dolomitic limestone (Obert 1981). These formations exhibit a monocline structure, inclined at an angle of 50° to the northwest and oriented in a N51° direction (Bougdal 2009). Slopes are characterized by a moderate to low gradients, are typically blanketed by substantial scree deposits. One key geological feature in this area is the presence of a left-lateral vertical fault along the eastern flank of the massif, with a N10° orientation. Structural features of the massif are significantly influenced by a persistent network of discontinuities, giving rise to vulnerable rock blocks susceptible to fracturing (Zerzour et al. 2020). Additionally, the cliff is subject to a series of sub-vertical collapse faults that extend downstream and culminate in meter-scale cavities, aligned in a N120° to N145° direction (Fig. 1). Climatic characteristics of the study area are distinctively Mediterranean in nature (Ncibi et al. 2021; Benmarce et al. 2021, 2023). The study region receives one of the highest average annual precipitations in Algeria; with an annual average of 892 mm. Rainfall is at its peak

during the period from October to April, coinciding with the season when rockslides are most likely to occur. Conversely, the lowest precipitation levels are observed between May and September. Furthermore, the presence of karstification in the Cap Aokas limestone massif significantly enhances its permeability, facilitating the infiltration and storage of groundwater.

2.2 Data collection

In our investigation of rockfall hazards in mountainous rocky cliffs, thorough data collection was crucial for grasping the geological and structural nuances of the study area. We digitized the Ziama geological map N48° and conducted on-site surveys in accessible locations. These field studies involved identifying and mapping lithological formations and utilized the scanline and window methods (Netshilaphala and Zvarivadza 2022) to measure and describe the dip, dip direction of discontinuities,

persistence, and spacing, following the approach recommended by ISRM (2021). Additionally, we analyzed geotechnical properties like wet density values and average uniaxial compressive strength to deepen our understanding of rock mass characteristics.

To incorporate topographic details, a topographic survey using photogrammetry was carried out following the method outlined by Hyslop et al. (2021). Survey conducted by IMSRN (engineering consultancy for Soil Movement and Natural Risks Engineering) in 2016 involved the use of 800 helicopter photos. Photographs were mainly taken horizontally, but some were angled downward. Resulted in a detailed point cloud comprising 32 million points, complemented by 13 ground control points for accuracy. Subsequently, survey data was transferred to ARCGIS10.8 software. There, we processed the vector data into raster data, creating a Digital Elevation Model (DEM) with a resolution of 5 meters (Hadji et al. 2016, 2017) (Fig. 3).

2.3 Kinematic analysis

For the examination of the structural features, we conducted a kinematic analysis methodology used by Hoek and Bray (1981), Goodman (1989), and Wyllie and Mah (2004). Additionally, we utilized Dips 7.0 software (Rocscience 2019) for our analysis. This software enabled the analysis and visualization of structural data based on dip and dip direction. We projected the discontinuity survey points stereographically to identify primary joint sets in the study area, as suggested by Keskin and Polat (2022). This analysis factored in the average direction and angle of friction of the cliff to select possible failure combinations, drawing from the methodology outlined by Zahri et al. (2016) and Zeqiri et al. (2019). Discontinuities with small persistence and spacing were excluded from the study due to their tendency to produce blocks of reduced volume, as noted by Wang et al. (2022).

Kinematic analysis is conducted for the planar failure mode without applying lateral boundaries. This implies that the entire area is regarded as cinematically valid, considering the local topographic variations caused by the faults in family 7, thereby presenting the most adverse scenario. Conversely, a lateral constraint of 30° is established for the direct toppling mode, referencing the studies by Goodman (1980).

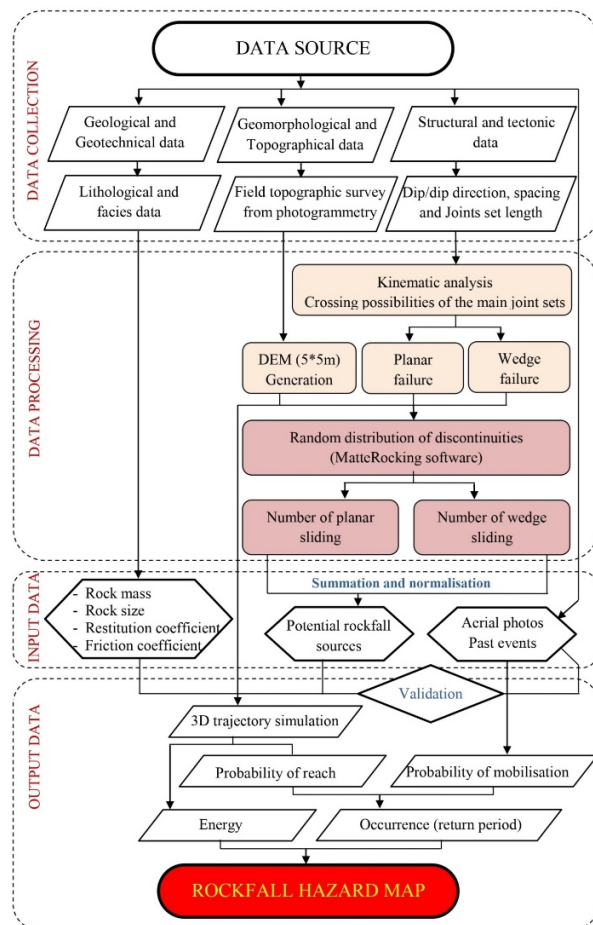## 2.4 Identification of rockfall source areas

Fig. 3 Methodological flowchart of the adopted approach.

Following Matterock's approach, which posits that rock mass discontinuities are a key factor in rock instabilities (Derron et al. 2005), we aimed to identify areas susceptible to plane or wedge failure modes. This method involves comparing the slope and orientation of each cell in the numerical model with the characteristics of discontinuities (dip/dip direction). To pinpoint areas prone to rockfall, we conducted a kinematic analysis for every section of the Digital Elevation Model (DEM). This analysis involved determining the average likelihood of planar or wedge failures and visualizing their spatial patterns across the slope (Fig. 4a, 4b). Furthermore, we assessed the susceptibility to movement, indicating the concentration of structural weaknesses (Fig. 4c). This density measure was derived from standardizing the total count of potential planar and wedge failures.

To facilitate this identification, we employed the Matterocking software, which relies on the DEM resolution, as recommended by Kakavas and Nikolakopoulos (2021).
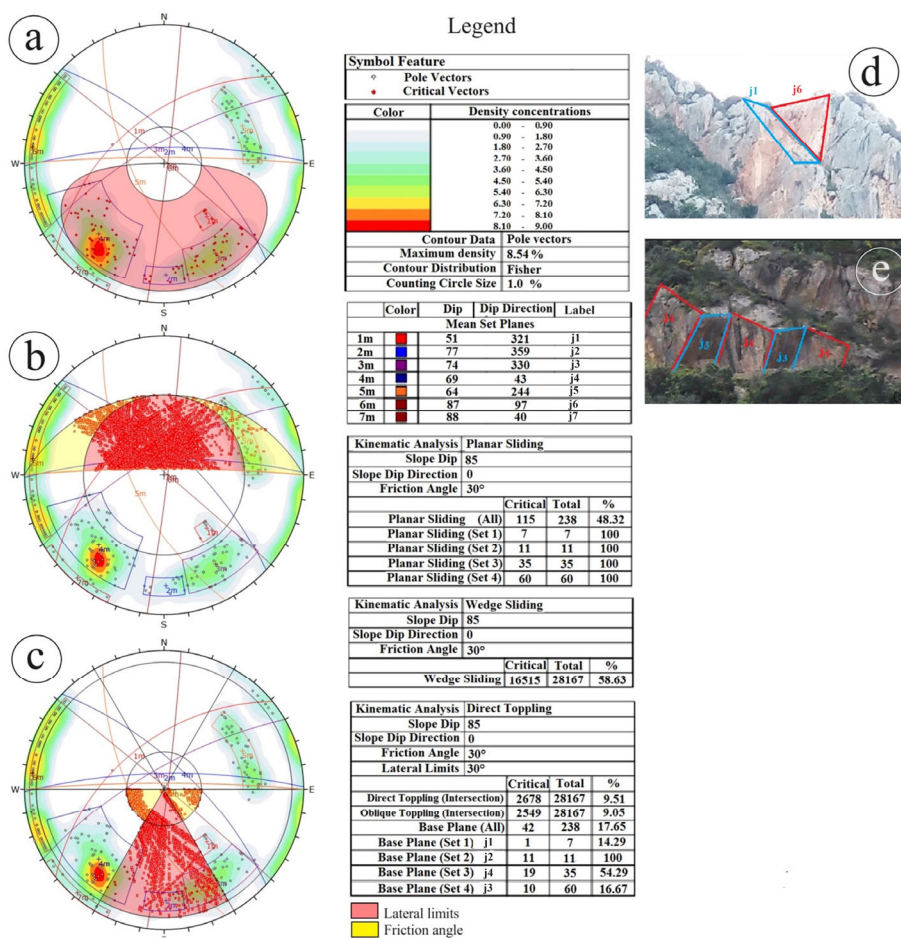
Fig. 4 Kinematic analysis of the Cap Aokas cliff; (a) Planar sliding, (b) Wedge sliding, (c) Direct toppling, (d) Wedge caused by (j1-j6) discontinuities, (e) Wedge caused by (j3-j4) discontinuities.

2.5 Trajectory simulation in 3D

For analyzing the trajectory of falling blocks, we utilized a 3D probabilistic model based on Bayesian analysis, which assesses the likelihood of occurrence given specific events. This approach treats model parameters as random variables. We estimated plausible ranges of results (mean, standard deviation, etc.) from the modelling process and assigned a probability distribution to them. Essentially, this is a statistical method founded on observations of random occurrences, leveraging the governing laws to analyze past phenomena or forecast future events.

Random number generation process adheres to a true random strategy, ensuring that each new calculation results in probabilistic simulations that cannot be replicated or repeated. For the simulation of block distribution and associated characteristics like velocity, frequency, rebound, height, kinetic energy,

time, impact, and stopping point, we followed the methodologies outlined by Fanos and Pradhan (2018, 2019). This simulation integrated data from the Digital Elevation Model (DEM), block properties (such as initial position, mass, dimensions, and initial velocity), and soil properties (including friction coefficient, normal and tangential restitution coefficients, lateral deviation, flattening, and rebound angle). These parameters were determined based on RocPro 3D software's features, customized to suit the terrain characteristics of our study area. Our adjustments were guided by relevant literature sources, including studies by Lan et al. (2007); Sarro et al. (2014, 2018, and 2020); Mateos et al. (2016); and He et al. (2020).

Trajectory simulation includes three phases: free fall, rolling/sliding, and impact, treating blocks as rigid bodies to consider rotation during movement. It adheres to the general dynamic equilibrium equation for translational failures. During free fall, air friction is negligible, and block rotation doesn't affect kinematics. Upon surface interaction, kinematics transition to rolling with friction but no sliding. Impact ends movement instantly, dissipating energy, while rotational velocity's influence is factored (Zhang et al. 2021).

RocPro3D software, a practical tool considering soil characteristics and terrain irregularities through a probabilistic approach (Akin et al. 2021), was employed for 3D modelling of trajectories. The software represented block parameters as uniform probabilistic variables and soil parameters as Gaussian or uniform probabilistic variables using the probabilistic model (Gallo et al. 2021). Triangulation allowed RocPro3D to generate a three-dimensional terrain mesh, facilitating the simulation of lateral

trajectory evolution, (Morales et al. 2021).

To simulate rockfall occurrence, we evenly distributed source points along the source line at 1-meter intervals. At each source point, ten blocks were projected in different directions, each with an initial velocity of 0.5 m/s, representing the long-term rockfall conditions (San et al. 2020). This velocity value is considered precautionary, as emphasized by Fanos et al. (2020). The simulation, performed using a 3D probabilistic model with a rigid block trajectory formulation on the digital terrain model mesh, generated multiple maps, including the trajectory frequency map and the kinetic energy map. Finally; we performed the Kolmogorov-Smirnov test to evaluate the normality of the empirical curve relative to the analytical curve. This test is employed to examine the sensitivity of probabilistic trajectory simulation, affirming that the parameters integrated into the simulation are genuine random variables.

2.6 Evaluating the rockfall hazard

To assess the rockfall hazard at specific locations, we applied the Matterock methodology, which considers the probability of occurrence, mobilization, and energy of the rock blocks. This approach involves pairing the probability of occurrence (expressed as a return period in years) with the intensity of the hazard (measured in kJ), as described by Hantz et al. (2021) and Ferrari et al. (2017).

Evaluation of rockfall hazard relies on assessing the kinetic energy "E," a critical factor in determining impact energy within the exposed zone. This energy encompasses both the translational and rotational energies of a rock block along its trajectory, defining its intensity (Lateltin et al. 2005; Prina Howald and Abbruzzese 2022). This intensity classification

corresponds to the structural capacity of various building walls to withstand impact energy, as demonstrated by Eggers et al. (2021). They categorized the intensity into three levels for simplification: high, medium, and low (Fig. 5), with a threshold of 300 kJ marking the boundary between high and medium classes, and 30 kJ representing the upper limit for the low-energy class (Mineo 2020). For precise hazard mapping, we employed the modified Matterocking method, analyzing 90% of the total simulated blocks to estimate the energy profile (Abbruzzese et al. 2009).

Probability of occurrence is determined by time intervals where an event has a high likelihood of happening (OFEFP 1997). It is qualitatively assessed according to Fig. 6, considering both its probability of failure and probability of reach. The probability of reach indicates the proportion of blocks starting from a point and reaching various locations within the study area. Return periods (T) were calculated as the inverse of occurrence frequency (f) [$T = 1/f$], (Jaccard et al. 2020). In simpler terms, higher frequency corresponds to shorter return periods. Finally, three levels of intensity, high, medium, and low, are used with the corresponding return periods of 1–30, 30–100, and 100–300 years to assess rock fall hazard. Hazard levels for each DEM cell was evaluated based on the (E, T) (Energy/Return period) pair and depicted on a frequency-intensity diagram (Abbruzzese and Labiouse 2020).

3 Results and Discussions

3.1 Data collection and kinematic analysis

Five discontinuity families (j2, j3, j4, j5, j6) were identified through stereographic projection of the

a		Probability of mobilization (Pm)			b		Return Period (T)		
Probability of occurrence (Pr\Pm)		High (Pm)	Moderate (Pm)	Low (Pm)	Rock fall hazard (E\T)		High (30 years)	Moderate (100 years)	Low (300 years)
Probability of reaching (Pr)	High (Pr > one event in 10 years period) [1 %]	High	High	Moderate	Energy (E)	High (E > 3000 kj)	High	High	Moderate
	Moderate (Pr = one event in 10 to 100 years period) [10^{-2} %]	High	Moderate	Low		Moderate (E = 300 to 3000 kj)	High	Moderate	Low
	Low (Pr < one event in 100 years period) [10^{-4} %]	Moderate	Low	Low		Low (E < 300 kj)	Moderate	Low	Low

Fig. 5 (a) Probability of the occurrence of rockfall hazard, (b) the pairwise matrix of rockfall hazard (Swiss directive from OFAT, OFEE, OFEFP, 1997).

discontinuity survey, excluding the bedding plane (j1) and fault series (F7). Stratification joints (j1) are less visible in the eastern part due to the dense dolomitic limestone appearance, but they're more evident in the western part where dolomitic limestones are bedded. Accessibility and vegetation cover influenced measurement availability. Family 7 comprises six sub-parallel faults crossing the slope from bottom to top (Fig. 3), significantly impacting the slope's ruggedness, mainly from a geomorphological perspective. The discontinuity sets (j2, j3, j4, j5, j6) play a role in rock mass fragmentation and weakening, clearly indicating potential rupture planes such as planar, wedge, and/or direct toppling (Table 1). For a friction angle of $\varphi = 30°$, the kinematic analysis allowed us to distinguish three failure modes (plane, wedge and direct toppling).

In the planar failure mode, the discontinuity families j1, j2, j3, and j4 are involved. The onset of failure for J1 occurs at slopes greater than or equal to 56°. However, j2, j3, and j4 show sliding potential at slopes ranging from 75° to 78°. The wedge failure mode is observed in 15 intersection cases, out of which 12 demonstrate possible failure scenarios. The initiation of failure occurs at slopes greater than 40° (Table 2). Discontinuity families susceptible to direct toppling comprise j1, j2, j3, and j4. Among them, j2 shows the highest susceptibility to direct toppling at 100%, whereas j4 is moderately susceptible at 54%. In contrast, j1 and j3 exhibit the lowest susceptibility to direct toppling, with probabilities of 14% and 16%, respectively. In our study, we implemented quality control measures throughout the data collection and kinematic analysis phases to ensure accuracy and reliability. During data collection, we strictly followed standardized protocols that specified data types, units of measurement, and procedures to maintain consistency. We conducted regular calibration of measurement equipment, including laser rangefinders, GPS devices, and inclinometers, to ensure accuracy. Data validation procedures, such as checks against acceptable ranges and the use of electronic data logging systems, were employed to minimize errors. Additionally, we took duplicate measurements for critical parameters to enhance reliability. Furthermore, we recorded weather and environmental conditions to account for external influences on the data. In the kinematic analysis phase, we upheld data verification standards to ensure completeness and address any missing or inconsistent data. We consistently applied a reliable and validated method for analysis. Regular
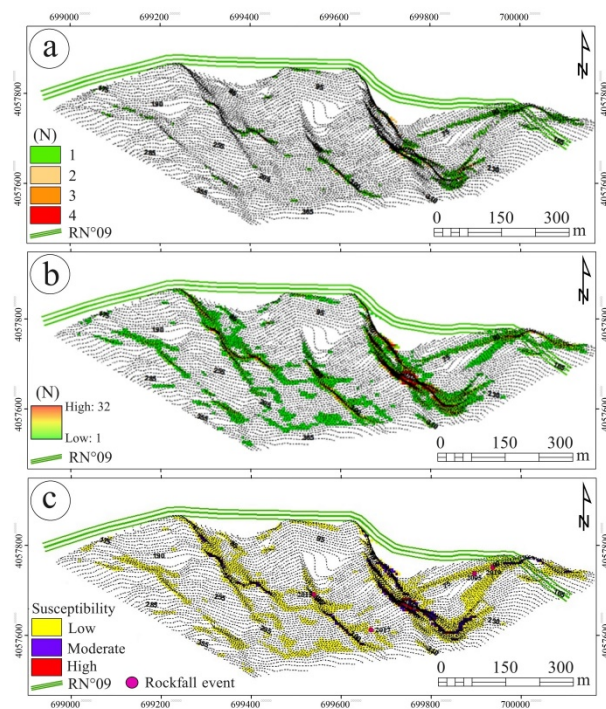

Fig. 6 (a) Average number of discontinuities of planar failure, cases of (j1), (mean number of potential planar sliding along joint/DEM cell). (b) Average number of discontinuities of wedge failure cases of (j1-j6), (mean number of potential wedge sliding along intersection j1-j6). (c) Susceptibility map for rockfall mobilization of the Aokas Cap cliff.

Table 1 Geometric characteristics of discontinuities.

Sets	j1	j2	j3	j4	j5	j6	F7
Dip (°)	51	77	69	74	64	87	88
Dip Direction (°N)	321	359	43	330	244	90	40
Direction (°N)	51	89	133	60	334	187	130
Mean spacing	3	1	1	1	1	2	300
Mean trace length (m)	15	1.2	1.5	1	0.8	8	> 50

Table 2 Minimum slopes causing failure of each wedge

Slope	Possible wedges
41° - 52°	(j1- j6); (j1- j4)
65° - 71°	(j4- j6); (j5- j1); (j4- j3); (j6- j3)
77° - 90°	(j4- j2); (j2- j3); (j2- j5); (j2- j6); (j2- j1); (j3- j5)

sensitivity assessments were conducted to evaluate the impact of errors or uncertainties.

3.2 Identification of areas of origin for rockfall

Presence of a certain number of discontinuities on a topographic surface corresponds to a probability ($P = 1 - e^{-N}$) of a hazardous structure existing, where N represents the average number of discontinuities

Table 3 Geotechnical characteristics of the terrain

Lithology	RN	RT	DL	Dv	K	β-lim	β-lim'
Dolomitic limestone	0.67	0.88	10	1	0.4	4°	30°
Compact slope debris	0.45	0.70	7.5	1	0.6	6°	40°

Note: RN and RT: Respectively normal and tangential restitution coefficients; DL and DV: Respectively lateral deviation, flattening; K: Friction coefficient. β-lim and β-lim': Rebound angles.

Fig. 7 Geographic position of Cap Aokas cliff, and photograph of detached blocks located on N130° oriented.
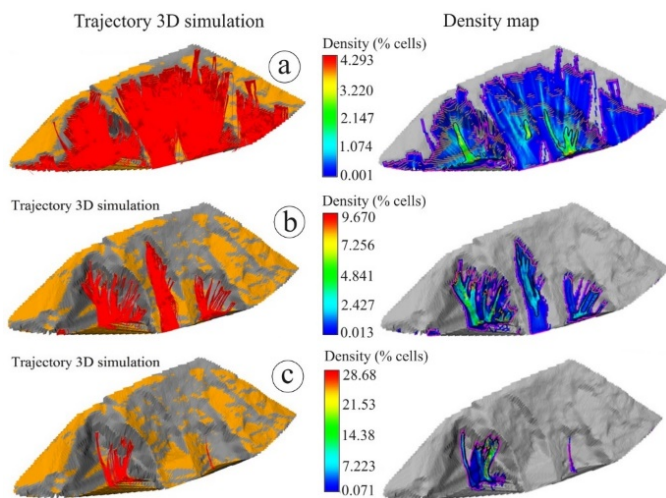

Fig. 8 3D simulation of trajectories and density maps from source zones for: (a) low, (b) medium, (c) high.

observed over a distance or area. Therefore, as the number N of discontinuities increases, the likelihood of hazardous structures being present also rises, approaching 100% (for $N = 1$, $F \approx 63\%$; for $N = 3$, $F \approx 95\%$; and for $N = 4.6$, $F \approx 99\%$). Consequently, the susceptibility to failure increases.

Susceptibility map shows that the red zones are indicative of high potential for mobilization, primarily concentrated on very steep slopes ($\geq 75°$) facing northeast. Areas of moderate mobilization are situated on slopes ranging from 65° to 75°, facing northeast and northwest. On the other hand, low mobilization areas are found on slopes ranging from 50° to 65°, facing northeast to northwest. Additionally, the source areas for some significant past events are projected to coincide with the mobilization potential areas on the established map (Fig. 5c). Aerial measurements (Fig. 6) further demonstrates that the traces of detached blocks match the spatial distribution of areas with moderate to high mobilization potential.

3.3 Simulating trajectories in 3D

Using a probabilistic approach, we conducted 3D simulations of trajectories based on lithology-related parameters (Table 3). These simulations enabled the calculation of density, stopping point, rebound height, velocity, and kinetic energy for all detached blocks.

Blocks' trajectories exhibit a distinct orientation along topographic corridors that converge towards the base of the slope (Fig. 7). Notably, some of these blocks extend to the downstream national road RN°9.

Zones where blocks come to a stop are characterized by the highest trajectory densities (Fig. 8), with the highest frequency observed in areas with high mobilization potential, reaching up to ($D_{low-mob} = 4.293\%$, $D_{Moderate-mob} = 9.67\%$, $D_{High-mob} = 28.68\%$) (Fig. 8). This indicates that a higher number of stopping points are observed in areas with a higher frequency of block passage. By reclassifying and overlaying the attainment maps of the three mobilization zones (low,
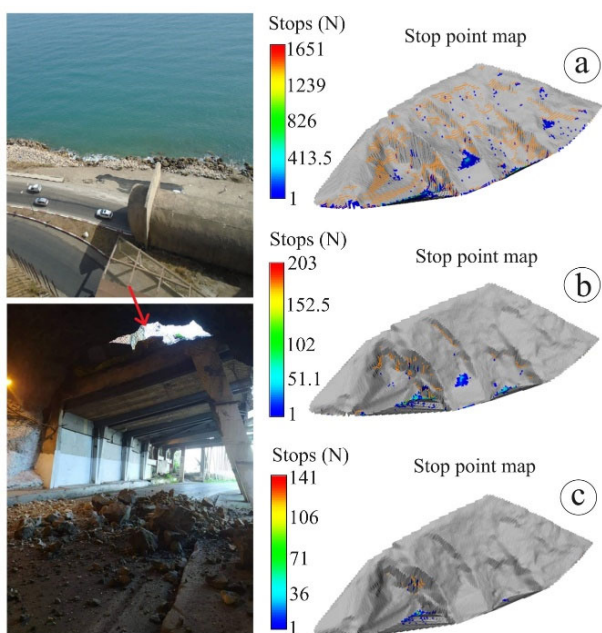
Fig. 9 Photo of rockfall occurred in 2019, with blocks reaching the tunnel western exit; Stopping point densities for mobilization zones: (a) low, (b) medium, (c) high.

heights.

Obtained energies in the simulation were influenced by various factors, including the initial conditions (such as initial velocity and density), lithological properties of the terrain, and the topography of the area.

We categorize the stretched Energy (Fig. 11c) in 3 classes (Fig. 11d). The highest energy class (class 3) with values greater than 300 kJ was attained when blocks underwent free fall during their trajectories (Fig. 12a). This class covered the largest area of the cliff (71.2%). The energy class 2, ranging between 30 and 300 kJ, was associated with slope gradients between 50° and 65°, and blocks did not experience free fall during their trajectories (Fig. 12b). This class was distributed around the periphery of class 3 and accounted for 27% of the affected area. The energy class 1, where the energy was less than 30 kJ, was found to be minimal (1.88%) and was mainly located in the western limit of the cliff (Fig. 12c). This class was associated with areas where the slope was less than 50°,
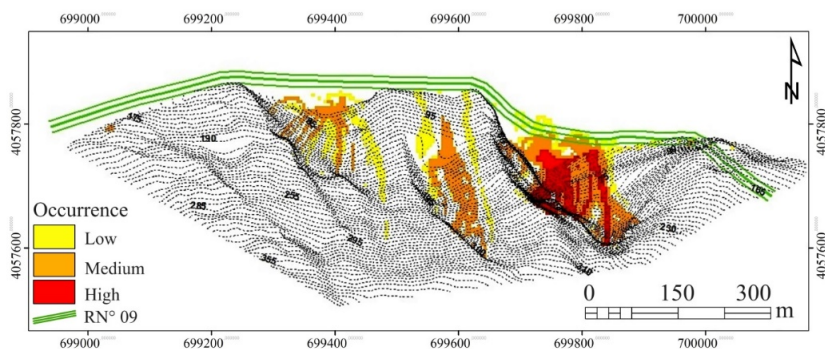
medium, and high) based on Fig. 5, stopping densities for mobilization zone were generated (Figs. 9a, b, c).

Based on the occurrence map, the high occurrence zone covers 17% of the attainment area, whereas the medium occurrence zone represents 52.44%, and the low occurrence zone covers the remaining 30%. For the analysis of kinetic energy, velocity, and rebound height, a 90% quintile was used to represent the statistical parameters of the cell grid populations (Fig. 10).

Distribution of velocities is consistent with that of rebound heights throughout the cliff (Fig. 11a). This suggests a correlation between the slope gradient and the velocity of the blocks in motion. In areas with steep slopes, the velocity and rebound height reach maximum values at the point of impact, after a free fall (Fig. 11b). As a result, higher fall heights lead to greater velocities and rebound

Fig. 10 Rockfall occurrence probability map of Cap Aokas cliff.
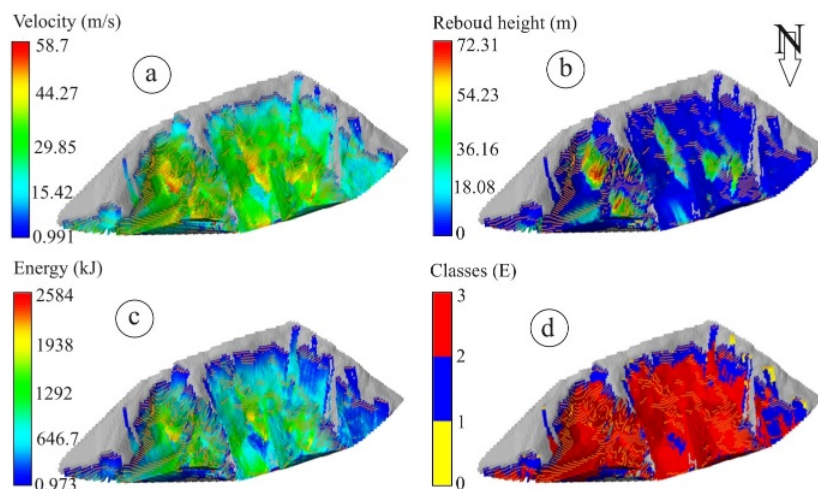

Fig. 11 3D simulation maps: (a) Velocity map [Envelope (Q-90)]; (b) Rebound height; (c) Energy map; (d) Energy class map.

and the velocity of the blocks was relatively low, ranging between 2.25-5 m/s.

Sensitivity test produced a distribution map of KS-p values (Fig. 13), indicating complete adherence of the simulation to a normal distribution. This is evidenced by the KS-p value obtained being greater than or equal to 5%.

This means that the trajectory simulation based on a probabilistic approach is well-founded, and its sensitivity concerning this approach has been verified. The results obtained from the trajectory simulation are further scrutinized and validated in the field through a retrospective analysis of events affecting the study area during specific periods (e.g., 2005, 2015, and 2019). Here, we observed a typical coherence between the block endpoints and the probability of impact points obtained through simulation.

3.4 Assessment of the rockfall hazard

In a particular area, rock fall hazard pertains to the likelihood of a rock fragment breaking away and reaching a specific zone within a defined time window, factoring in its energy and vertical distance (Hantz et al. 2021). Consequently, evaluating rockfall hazard involves considering various factors and is categorized according to Swiss standards (OFEFP 1997) using the ratio of magnitude (energy/return period). By performing a raster calculation of energy and return period, it was possible to create a hazard map (Fig. 14). Slopes predominantly exhibit energy class 3 (>300 kJ), implying that kinetic energy plays a more significant role in the hazard classification than the frequency of occurrence (return period). High hazard zone is concentrated between areas with very steep slopes and encompasses most of the affected zone. In contrast, the medium and low hazard zones are situated in the lower parts of the slope and regions with a low slope gradient. Notably, the National Road No. 9,

positioned downstream of the cliff, is highly susceptible to sections with elevated hazards, particularly from the western exit of the tunnel to approximately 560m.

3.5 Discussions

The kinematic analysis conducted in this study played a crucial role in identifying the failure mechanisms and source zones based on photogrammetry and high-resolution DEMs. Three failure modes were identified: planar, wedge, and direct toppling. However, it is worth noting that direct toppling was not observed in the field due to the presence of elongated rectangular blocks at the base, which prevented this mode of failure from occurring. Our analysis primarily focused on assessing failure possibilities influenced by slope angle, joint

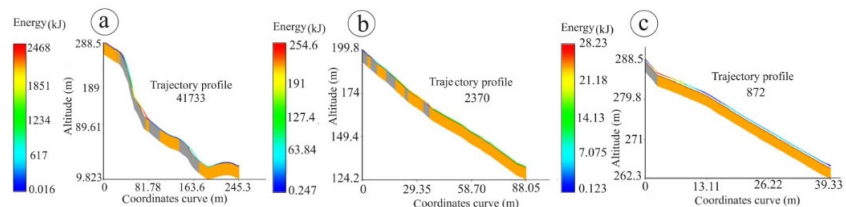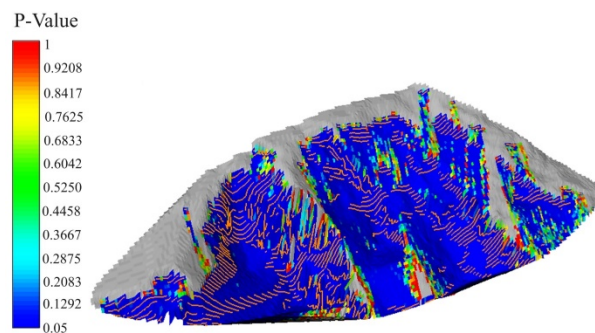**Fig. 12** Trajectory profiles of the class E3, E2, E1. (a) class-E3 (High); (b) class-E2 (Moderate); (c) class-E1 (Low).

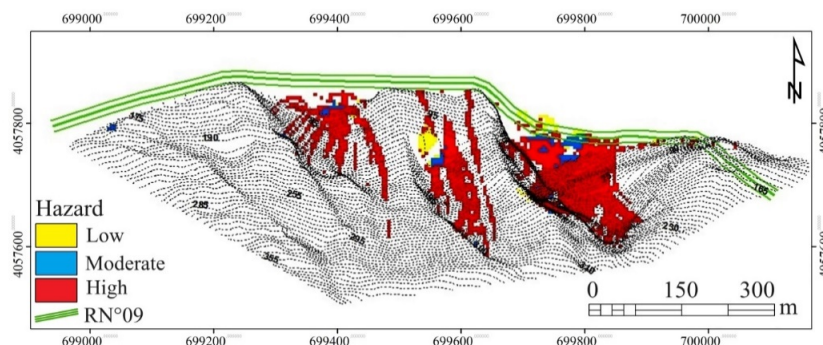**Fig. 13** P values of the Kolmogorov-Smirnov (KS-p) test.

Fig. 14 Rockfall hazard probability map of Cap Aokas cliff.

orientation, and slope orientation. The decision to conduct the kinematic analysis without lateral boundaries was supported by the spatial distribution of discontinuity families that were prone to plane failure across the slope.

To identify hazardous geological structures, we employed the Matterocking method, which revealed a distinct distribution of source zones along fault mirrors. This distribution was attributed to the influence of these faults on the slope's morphology. The alignment between the identified source zones and previously recorded events confirmed the accuracy of our findings. Trajectory simulation considered lateral dispersion and utilized a probabilistic model to account for uncertainties. The RocPro3D software was employed to analyze rockfall trajectories, taking into account factors such as velocity and energy.

While our methodology for assessing rockfall hazards was comprehensive, it is important to acknowledge potential sources of uncertainty and limitations. Uncertainties may arise from variations in field measurements, data collection methods, DEM generation, and assumptions made during the kinematic analysis and trajectory simulation. Additionally, the Matterock methodology has limitations in addressing direct toppling failures, and the probabilistic modelling approach may not fully capture the complexity of real-world scenarios. These uncertainties and limitations should be carefully considered when interpreting the results and making decisions regarding rockfall hazard mitigation.

The practical implications of our research are significant. It provides a comprehensive understanding of rockfall dynamics and hazards in the Aokas region, thereby aiding in risk assessment and management. The identification of specific discontinuity families and their failure modes offers valuable insights for infrastructure planning and design in rocky, mountainous areas. The research contributes to more accurate hazard mapping, particularly for critical transportation routes such as National Road No. 9. Furthermore, the study emphasizes the importance of considering geological structures and their influence on slope morphology when assessing rockfall hazards. The incorporation of a probabilistic approach sets a methodological precedent for more precise assessments in diverse geological settings.

This study has yielded significant findings regarding the rockfall hazards present in the Cap Aokas cliff region. Through a comprehensive examination of the region's geological characteristics, failure mechanisms, and the spatial distribution of source zones, we have gained valuable insights that can inform the development of effective rockfall hazard mitigation strategies.

4 Conclusions and Recommendations

In conclusion, the occurrence of rockfall events poses significant risks to rocky slopes and cliffs, necessitating a thorough assessment of rockfall hazards. Our research has shed light on the importance of evaluating both localized and diffuse components of rockfall hazards through various stages, including kinematic analysis and trajectory simulations. The influence of faults on slope morphology and the spatial distribution of source zones were identified as crucial factors determining rockfall occurrences.

To effectively mitigate the risks associated with rockfall, it is imperative to implement suitable protection measures. These measures should take into account the specific morphology of the site and consider the energy associated with falling blocks. By understanding the failure mechanisms and identifying vulnerable areas, appropriate engineering solutions such as protective barriers, slope stabilization techniques, or controlled rock removal can be implemented to minimize the potential impact of rockfall events.

However, it is important to acknowledge the limitations and uncertainties inherent in rockfall hazard assessments. Our study has highlighted some of these limitations, including uncertainties arising from field measurements, data collection methods, and assumptions made during analysis. Methodological refinements and ongoing research are necessary to further enhance our understanding of rockfall hazards and improve the accuracy of assessments in similar geological settings.

Looking ahead, it is recommended to continue studying and monitoring rockfall hazards in the Cap Aokas cliff region and other similar areas. Long-term monitoring programs can provide valuable data on the frequency and magnitude of rockfall events, aiding in the refinement of hazard models. Additionally, advancements in remote sensing technologies and data processing techniques can contribute to more accurate hazard mapping and early warning systems.

Furthermore, collaboration between researchers, geotechnical engineers, and local authorities is crucial for effective rockfall hazard management. Sharing knowledge and experiences can facilitate the development and implementation of comprehensive strategies to mitigate rockfall risks. Public awareness campaigns and educational programs can also contribute to enhancing safety measures and promoting responsible behavior in areas prone to rockfalls.

Acknowledgments

Author Contribution

LADJEL Zohra: Investigation, Methodology, Writing-original. ZAHRI Farid: Writing-review & editing, Data curation. HADJI Riheb: Supervision, Visualization, Writing-review and editing. Zighmi Karim: draft, Conceptualization. Hamed Younes and Kaddour Benmarce: Conceptualization, Formal analysis, Supervision.

Ethics Declaration

Availability of Data/Materials: The datasets generated during this study are available from the corresponding author upon reasonable request and within the framework of cooperation agreements and scientific research projects.

Conflict of Interest: The authors declare no conflict of interest.

References

Abbruzzese JM, Labiouse V (2020) New Cadanav methodology for rock fall hazard zoning based on 3D trajectory modelling. Geosciences 10(11): 434. https://doi.org/10.3390/geosciences10110434

Abbruzzese JM, Sauthier C, Labiouse V (2009) Considerations on Swiss methodologies for rock fall hazard mapping based on trajectory modelling. Nat Hazards Earth SystSci 9(4):1095-1109. https://doi.org/10.5194/nhess-9-1095-2009

Achour Y, Boumezbeur A, Hadji R, et al. (2017) Landslide susceptibility mapping using analytic hierarchy process and information value methods along a highway road section in Constantine, Algeria. Arab J Geosci 10(8): 194. https://doi.org/10.1007/s12517-017-3049-9

Akin M, Dinçer I, Ok AÖ, et al. (2021) Assessment of the effectiveness of a rockfall ditch through 3-D probabilistic rockfall simulations and automated image processing. Eng Geol 283. https://doi.org/10.1016/j.enggeo. 2021.106001

Anis Z, Wissem G, Riheb H, et al. (2019) Effects of clay properties in the landslides genesis in flysch massif: Case study of AïnDraham, Northwestern Tunisia. J Afr Earth Sci 151: 146-152. https://doi.org/10.1016/j.jafrearsci. 2019.01.011

Ansari MK, Ahmad M, Singh R, et al. (2018) 2D and 3D rockfall hazard analysis and protection measures for Saptashrungi Gad Temple, Vani, Nashik, Maharashtra – A Case Study. J GeolSoc India 91: 47-56. https://doi.org/10.1007/s12594-018-0902-9

Asmoay AA, Mabrouk WA (2023) Appraisal of rock-water interaction and frailty of groundwater to corrosion and salinization, Northwestern Gulf of Suez, Egypt. J Umm Al-Qura Univ Appl Sci 1-12. https://doi.org/10.1007/s43994-023-00075-0

Benmarce K, Hadji R, Zahri F, et al. (2021) Hydrochemical and geothermometry characterization for a geothermal system in semiarid dry climate: The case study of Hamma Spring (Northeast Algeria). J Afr Earth Sci 182: 104285. https://doi.org/10.1016/j.jafrearsci.2021.104285

Benmarce K, Hadji R, Hamed Y, et al. (2023) Hydrogeological and water quality analysis of thermal springs in the Guelma Region of North-Eastern Algeria: A study using hydrochemical, statistical, and isotopic approaches. J Afr Earth Sci 205: 105011. https://doi.org/10.1016/j.jafrearsci.2023.105011

Besser H, Dhaouadi L, Hadji R, et al. (2021) Ecologic and economic perspectives for sustainable irrigated agriculture under arid climate conditions: An analysis based on environmental indicators for Southern Tunisia. J Afr Earth Sci 177: 104134. https://doi.org/10.1016/j.jafrearsci.2021.104134

Boubazine L, Boumazbeur A, Hadji R, et al. (2022) Slope failure characterization: A joint multi-geophysical and geotechnical analysis, case study of Babor Mountains Range, NE Algeria. Min Mineral Depos 16(4). https://doi.org/10.1007/978-3-030-68747-5

Bougdal R (2009) Doubling of the Cap Aokas tunnel, synthesis of geological and geotechnical data. Geological Report (Internal document).

Brahmi S, Fehdi C, Hadji R, et al. (2023) Karst-induced sinkhole detection using a tomography imaging survey, case of Setifian high plain, NE Algeria. Geotech Geol Eng 41(3): 1961-1976. https://doi.org/10.1007/s10706-023-02384-x

Chibani A, Hadji R, Younes H (2022) A combined field and automatic approach for lithological discrimination in semi-arid regions, the case of geological maps of bir later region and its vicinity, Nementcha mounts, Algeria. Geomat Land manag Landsc (4). http://doi.org/10.15576/GLL/2022.4.7

Corominas J, Matas G, Ruiz-Carulla R (2019) Quantitative analysis of risk from fragmental rockfalls. Landslides 16(1): 5-21. https://doi.org/10.1007/s10346-018-1049-9

Cruden DM, Varnes DJ (1996) Landslide types and processes. In Turner AK, SchusterRL (Eds.), Landslides: Investigation and Mitigation (pp. 36-75). Transp Res Board Spec Rep No. 247.

NatlAcad Press. https://doi.org/10.17226/4917

Dahoua L, Yakovitch SV, Hadji R, et al. (2017) Landslide susceptibility mapping using analytic hierarchy process method in BBA-Bouira region, case study of East-West Highway, NE Algeria. In: Kallel A, Ksibi M, Ben Dhia H, et al. (eds.), Recent advances in environmental science from the Euro-Mediterranean and surrounding regions. EMCEI 2017. AdvSciTechnolInnov (IEREK InterdiscipSer Sustain Dev). Springer. pp 145-152.
https://doi.org/10.1007/978-3-319-70548-4_14

Dahoua L, Usychenko O, Savenko VY, et al. (2018) Mathematical approach for estimating the stability of geotextile-reinforced embankments during an earthquake. Min Sci 25: 207-217.
https://doi.org/10.5277/msc182501

Depountis N, Riquelme AJ, Abellán A, et al. (2020) Evaluation of the rockfall hazard using an unmanned aerial vehicle (UAV) and the displacement monitoring system: A case study in the Aosta Valley region (NW Italy). Eng Geol 277: 105764.
https://doi.org/10.1016/j.enggeo.2020.105764

Derron MH, Jaboyedoff M, Blikra LH (2005) Preliminary assessment of rockslide and rockfall hazards using a DEM (Oppstadhornet, Norway). Nat Hazards Earth SystSci 5(2): 285-292. https://doi.org/10.5194/nhess-5-285-2005

Descoeudres F (1997) Trajectory analysis of rockfalls. Int J Rock Mech Min Sci 34(3-4): 3-4.
https://doi.org/10.1016/S0148-9062(97)00054-7

Dorren L, Berger F (2013) 14. Modèles de trajectographie: atoutoucontrainte. In Lambert A, Tang AM, Jaboyedoff M (Eds.), Trajectoires des versants: processus, modélisation et surveillance. Presses Polytech Univ Romandes. pp 311-327.
https://doi.org/10.14375/NP.9782880747123.311

Eggers MJ, Nash T, Dwumfour D, et al. (2021) Natural slope hazard management and integration with mining operations ACG. pp 261-276. https://doi.org/10.36487/ACG_repo/2135_16

El Mekki A, Hadji R, Chemseddine F (2017) Use of slope failures inventory and climatic data for landslide susceptibility, vulnerability, and risk mapping in Souk Ahras region. Min Sci.
https://doi.org/10.5937/minsci1703065E

Fanos AM, Pradhan B (2018) Laser scanning systems and techniques in rockfall source identification and risk assessment: A critical review. Earth Syst Environ 2(2): 163-182.
https://doi.org/10.1007/s41748-018-0046-3

Fanos AM, Pradhan B (2019) A novel rockfall hazard assessment using laser scanning data and 3D modelling in GIS. Catena 172: 435-450. https://doi.org/10.1016/j.catena.2018.09.008

Fanos AM, Pradhan B, Alamri A, et al. (2020) Machine learning-based and 3D kinematic models for rockfall hazard assessment using LiDAR data and GIS. Remote Sens 12(11): 1755.
https://doi.org/10.3390/rs12111755

Ferrari F, Giacomini A, Thoeni K (2016) Qualitative rockfall hazard assessment: A comprehensive review of current practices. Rock Mech Rock Eng 49(7): 2865-2922.
https://doi.org/10.1007/s00603-016-0918-z

Ferrari F, Giacomini A, Thoeni K, et al. (2017) Qualitative evolving rockfall hazard assessment for highwalls. Int J Rock Mech Min Sci 98: 88-101.
https://doi.org/10.1016/j.ijrmms.2017.08.013

Fredj M, Hafsaoui A, Riheb H, et al. (2020) Back-analysis study on slope instability in an open pit mine (Algeria). Sci Bull Natl Min Univ. https://doi.org/10.33271/nvngu/2020-2/024

Gallo IG, Martínez-Corbella M, Sarro R, et al. (2021) An integration of UAV-based photogrammetry and 3D modelling for rockfall hazard assessment: The Cárcavos case in 2018 (Spain). Remote Sens 13(17): 3450.
https://doi.org/10.3390/rs13173450

Goodman RE (1980) Introduction to Rock Mechanics. (ed.). John Wiley & Sons, New York.

Goodman RE (1989) Introduction to Rock Mechanics (2nd ed.). Wiley, New York.

Hadji R, Boumazbeur A, Limani Y, et al. (2013) Geologic, topographic and climatic controls in landslide hazard assessment using GIS modeling: A case study of Souk Ahras region, NE Algeria. Quat Int 302 : 224-237.
https://doi.org/ 10.1016/j.quaint.2013.02.011

Hadji R, Limani Y, Demdoum A (2014) Using multivariate approach and GIS applications to predict slope instability hazard: Case study of Machrouha municipality, NE Algeria. In 2014 International Conference on ICT for Sustainable Development (ICT4SD). IEEE. pp 1-5.
https://doi.org/10.1109/ICT-DM.2014.6917787

Hadji R, Chouabi A, Gadri L, et al. (2016) Application of linear indexing model and GIS techniques for the slope movement susceptibility modeling in Bousselam upstream basin, Northeast Algeria. Arab J Geosci 9: 192.
https://doi.org/10.1007/s12517-015-2063-y

Hadji R, Raïs K, Gadri L, et al. (2017) Slope failures characteristics and slope movement susceptibility assessment using GIS in a medium scale: A case study from Ouled Driss and Machroha municipalities, Northeastern of Algeria. Arab J Sci Eng 42: 281-300.
https://doi.org/10.1007/s13369-016-2232-7

Hantz D, Dussauge-Peisser C, Jeannin M, et al. (2002) Rock fall Hazard: from expert opinion to quantitative evaluation. In Geomorphology: From Expert Opinion to Modelling. pp -115.
https://doi.org/10.1016/S0169-555X(02)00019-2

Hantz D, Corominas J, Crosta GB, et al. (2021) Definitions and concepts for quantitative rockfall hazard and risk analysis. Geosciences 11(4): 158.
https://doi.org/10.3390/geosciences11040158

Hoek E, Bray JD (1981) Rock slope engineering. CRC Press

Hudson JA (1992) Rock engineering systems: Theory and practice. Chapman and Hall.
https://doi.org/10.1007/978-94-011-2793-7

Hyslop A, Day JJ, Kruse S, et al. (2021) Numerical failure prediction of the Sentinel sea stack formation at Hopewell Rocks Provincial Park with input from UAV-based photogrammetry and erosion records. J Struct Geol 147 : 104346. https://doi.org/10.1016/j.jsg.2021.104346

He K, Li Y, Ma G, et al. (2021) Failure mode analysis of post-seismic rockfall in shattered mountains exemplified by detailed investigation and numerical modelling. Landslides 18: 425-446.https://doi.org/10.1007/s10346-020-01532-1

ISRM, International Society for Rock Mechanics (2021) Rockfall. In ISRM suggested methods for rock characterization, testing and monitoring: 2007-2014. CRC Press. pp. 47-48.
https://doi.org/10.1201/9781003095748-15

Jaboyedoff M, Philippossian F, Mamin M, et al. (1996) Distribution spatiale des discontinuités dans une falaise. Approche statistique et probabiliste, Rapport de travail PNR31, Hochschulverlag AG an der ETH Zürich.

Jaboyedoff M, Metzger R, Oppikofer T, et al. (2007) New insight techniques to analyze rock-slope relief using DEM and 3D imaging cloud points: COLTOP-3D software. 1st Canada-US Rock Mechanics Symposium. OnePetro.
https://doi.org/10.2118/110951-MS

Jaccard CJ, Abbruzzese JM, Howald EP (2020) An evaluation of the performance of rock fall protection measures and their role in hazard zoning. Nat Hazards 104: 459-491.
https://doi.org/10.1007/s11069-020-04174-z

Jiang N, Li HB, Liu MS, et al. (2020) Quantitative hazard assessment of rockfall and optimization strategy for protection systems of the Huashiya cliff, southwest China. Geomat Nat Hazards Risk 11(1): 1939-1965.
https://doi.org/10.1080/19475705.2020.1829762

Kakavas MP, Nikolakopoulos KG (2021) Digital elevation models of rockfalls and landslides: a review and meta-analysis. Geosciences 11(6): 256.
https://doi.org/10.3390/ geosciences11060256

Kallel A, Ksibi M, Dhia HB, et al. (2018) Recent advances in environmental science from the Euro-Mediterranean and surrounding regions: proceedings of Euro-Mediterranean Conference for Environmental Integration (EMCEI-1), Tunisia 2017. Springer International Publishing.
https://doi.org/10.1007/978-3-319-70548-4

Karim Z, Hadji R, Hamed Y (2019) GIS-based approaches for the landslide susceptibility prediction in Setif Region (NE Algeria). GeotechGeolEng 37(1): 359-374.
https://doi.org/10.1007/s10706-018-0653-8

Kerbati NR, Gadri L, Hadji R, et al. (2020) Graphical and numerical methods for stability analysis in surrounding rock of underground excavations, example of Boukhadra Iron Mine NE Algeria. Geotech Geol Eng 38: 2725-2733.
https://doi.org/10.1007/s10706-019-01181-9

Keskin I, Polat A (2022) Kinematic Analysis and Rockfall Assessment of Rock Slope at the UNESCO World Heritage city (Safranbolu/Turkey). Iran J Sci Technol Trans Civ Eng 46(1): 367-384. https://doi.org/10.1007/s40996-021-00661-2

Lan H, Martin CD, Lim CH (2007) RockFall analyst: A GIS extension for three-dimensional and spatially distributed rockfall hazard modeling. Comp Geosci 33(2): 262-279.
https://doi.org/10.1016/j.cageo.2006.05.013

Lateltin O, Haemmig C, Raetzo H, et al. (2005) Landslide risk management in Switzerland. Landslides 2(4): 313-320.
https://doi.org/10.1007/s10346-005-0018-8

Mahdadi F, Boumezbeur A, Hadji R, et al. (2018) GIS-based landslide susceptibility assessment using statistical models: a case study from Souk Ahras province, NE Algeria. Arab J Geosci 11(17): 476. https://doi.org/10.1007/s12517-018-3771-8

Mahleb A, Hadji R, Zahri F, et al. (2022) Water-Borne Erosion Estimation Using the Revised Universal Soil Loss Equation (RUSLE) Model Over a Semiarid Watershed: Case Study of Meskiana Catchment, Algerian-Tunisian Border. Geotech Geol Eng 40(8): 4217-4230.
https://doi.org/10.1007/s10706-022-02152-3

Manchar N, Benabbas C, Hadji R, et al. (2018) Landslide Susceptibility Assessment in Constantine Region Algeria By Means of Statistical Models. Studia Geotech Mech 40(3): 208-219. https://doi.org/10.2478/sgem-2018-0021

Mateos RM, García-Moreno I, Reichenbach P, et al. (2016) Calibration and validation of rockfall modelling at regional scale: application along a roadway in Mallorca (Spain) and organization of its management. Landslides 13: 751-763.
https://doi.org/10.1007/s10346-015-0602-5

Mineo S (2020) Comparing rockfall hazard and risk assessment procedures along roads for different planning purposes. J Mt Sci 17(3):653-669. https://doi.org/10.1007/s11629-019-5766-3

Morales T, Clemente JA, Mollá LD et al. (2021) Analysis of instabilities in the Basque Coast Geopark coastal cliffs for its environmentally friendly management (Basque-Cantabrian basin, northern Spain). Eng Geol 283: 106023.
https://doi.org/10.1016/j.enggeo.2020.106023

Ncibi K, Hadji R, Hajji S, et al. (2021) Spatial variation of groundwater vulnerability to nitrate pollution under excessive fertilization using index overlay method in central Tunisia (SidiBouzid basin). Irrig Drainage 70(5): 1209-1226.
https://doi.org/10.1002/ird.2599

Netshilaphala V, Zvarivadza T (2022) Fall of ground management through underground joint mapping: shallow chrome mining case study. Geotech Geol Eng 40(4): 2231-2254.
https://doi.org/10.1007/s10706-022-02116-3

Obert D (1981) Geological study of the eastern Babors (Tell domain, Algeria) (Doctoral dissertation, Toulouse).

OFEFP (1997) Federal Office for the Environment, Forests and Landscape.

Palau J, Janeras M, Prat E, et al. (2013) Preliminary assessment of rockfall risk mitigation in access infrastructures to Montserrat. In Landslide Science and Practice: Volume 6: Risk Assessment, Management and Mitigation. pp 255-261.
https://doi.org/10.1007/978-3-642-31325-7_34

Prina Howald E, Abbruzzese JM (2022) A framework for assessing the performance capabilities of rock fall protections for hazard analysis and zoning. Appl Sci 12(17): 8834.
https://doi.org/10.3390/app12178834

Regione Lombardy (2000) Methods for analyzing rockfall risk and evaluating the effectiveness of mitigation measures. Department of the Environment, Geological and Geotechnical Sector, Geological, Seismic and Soil Service, Milan.

Rocscience R (2019) 2D software. Rocscience Inc., Toronto, Canada. https://doi.org/10.5281/zenodo.2651842

Saadoun A, Yilmaz I, Hafsaoui A, et al. (2020) Slope Stability Study in Quarries by Different Approaches: Case Chouf Amar Quarry, Algeria. In IOP Conference Series: Materials Science and Engineering. IOP Publishing. 960(4): 042026.
https://doi.org/10.1088/1757-899X/960/4/042026

San NE, Topal T, Akin MK (2020) Rockfall hazard assessment around Ankara Citadel (Turkey) using rockfall analyses and hazard rating system. Geotech Geol Eng 38: 3831-3851.
https://doi.org/10.1007/s10706-020-01261-1

Sarro R, Mateos RM, García-Moreno I, et al. (2014) The Son Poc rockfall (Mallorca, Spain) on the 6th of March 2013: 3D simulation. Landslides 11: 493-503.
https://doi.org/10.1007/s10346-014-0487-8

Sarro R, Riquelme A, García-Davalillo JC, et al. (2018) Rockfall simulation based on UAV photogrammetry data obtained during an emergency declaration: Application at a cultural heritage site. Remote Sens 10(12): 1923.
https://doi.org/10.3390/rs10121923

Sarro R, Maria Mateos R, Reichenbach P, et al. (2020) Geotechnics for rockfall assessment in the volcanic island of Gran Canaria (Canary Islands, Spain). J Maps 16(2): 605-613.
https://doi.org/10.1080/17445647.2020.1759373

Taib H, Hadji R, Hamed Y, et al. (2023a) Exploring neotectonic activity in a semiarid basin: a case study of the Ain Zerga watershed. J Umm Al-Qura Univ Appl Sci 1-14.
https://doi.org/10.1007/s43994-023-00072-3

Taib H, Hadji R, Hamed Y (2023b) Erosion patterns, drainage dynamics, and their environmental implications: a case study of the hammamet basin using advanced geospatial and morphometric analysis. J Umm Al-Qura Univ Appl Sci 1-16.
https://doi.org/10.1007/s43994-023-00096-9

Taib H, Hadji R, Hamed Y, et al. (2024) Integrated geospatial analysis for identifying regions of active tectonics in the Saharian Atlas, an review analysis of methodology and calculation fundamentals. J Afr Earth Sci 211: 105188.
https://doi.org/10.1016/j.jafrearsci.2024.105188

Tamani F, Hadji R, Hamad A, et al. (2019) Integrating remotely sensed and GIS data for the detailed geological mapping in semi-arid regions: case of Youks les Bains Area, Tebessa Province, NE Algeria. Geotech Geol Eng 37(4): 2903-2913.
https://doi.org/10.1007/s10706-019-01019-9

Vengeon JM (2001) Historical Geomechanics and Probabilistic Hazard Assessment. Rock Mech Rock Eng 34(1): 67-91.
https://doi.org/10.1007/s006030170026

Volkwein A, Schellenberg K, Labiouse V, et al. (2011) Rockfall characterisation and structural protection–a review. Nat Hazards Earth Syst Sci 11(9): 2617-2651.
https://doi.org/10.5194/nhess-11-2617-2011

Wang XY, Yin YC, et al. (2022) Microsimulation study on energy release and rock block ejection force of granite under different unloading conditions. Front Earth Sci 10.
https://doi.org/10.3389/feart. 2022.826487

Wyllie DC, Mah C (2004) Rock slope engineering. CRC Press.

Zahri F, Boukelloul M, Hadji R, et al. (2016) Slope stability analysis in open pit mines of Jebel Gustar Career, Ne Algeria – A multi-steps approach. Mining Sci 23: 137-146.
https://doi.org/10.5277/msc162312

Zeqiri RR, Riheb H, Karim Z, et al. (2019) Analysis of safety factor of security plates in the mine" Trepça" Stantërg. Mining Sci 26: 21. https://doi.org/10.5277/msc192602

Zerzour O, Gadri L, Hadji R, et al. (2020) Semi-variograms and kriging techniques in iron ore reserve categorization: application at Jebel Wenza deposit. Arab J Geosci 13(16): 1-10.
https://doi.org/10.1007/s12517-020-06235-5

Zhang JY, Li HB, Yang XG, et al. (2021) Quantitative assessment of rockfall hazard in post-landslide high rock slope through terrestrial laser scanning. Bull Eng Geol Environ 80(10): 7315-7331. https://doi.org/10.1007/s10064-021-02429-1